# Fabrication of InAlGaN/GaN High Electron Mobility Transistors on Sapphire Substrates by Pulsed Metal Organic Chemical Vapor Deposition *

Ru-Dai Quan(全汝岱), Jin-Cheng Zhang(张进成)**, Ya-Chao Zhang(张雅超), Wei-Hang Zhang(张苇航), Ze-Yang Ren(任泽阳), Yue Hao(郝跃)

*Key Laboratory of Wide Band-Gap Semiconductor Technology, School of Microelectronics, Xidian University, Xi'an 710071*

(Received 29 June 2016)

*Nearly lattice-matched InAlGaN/GaN heterostructure is grown on sapphire substrates by pulsed metal organic chemical vapor deposition and excellent high electron mobility transistors are fabricated on this heterostructure. The electron mobility is 1668.08 $cm^2/V{\cdot}s$ together with a high two-dimensional-electron-gas density of $1.43 \times 10^{13}$ $cm^{-2}$ for the InAlGaN/GaN heterostructure of 20 nm InAlGaN quaternary barrier. High electron mobility transistors with gate dimensions of $1 \times 50$ $\mu m^2$ and 4 $\mu$m source-drain distance exhibit the maximum drain current of 763.91 mA/mm, the maximum extrinsic transconductance of 163.13 mS/mm, and current gain and maximum oscillation cutoff frequencies of 11 GHz and 21 GHz, respectively.*

*PACS:* 81.05.Bx, 81.05.Ea, 81.16.Be, 85.30.Tv DOI: 10.1088/0256-307X/33/10/108104

GaN-based high electron mobility transistors (HEMTs) have been used widely in the rf and millimeter-wave power applications.[1,2] This kind of device is commonly manufactured by using AlGaN/GaN heterostructures which can be grown with high material quality. However, the AlGaN barrier suffers from tensile stress induced by the lattice-mismatch between the AlGaN barrier and the GaN channel which is detrimental to AlGaN/GaN HEMT performances. This weakness has limited the design of the heterostructure and applications of the devices.[3–5] To solve this issue, the ternary compound InAlN has been intensively investigated as an alternative barrier material.[6–8] For InN mole fraction of approximately 18%, InAlN is lattice-matched to GaN and can provide high sheet electron densities owing to its high spontaneous polarization. Although the InAlN-based heterostructures have realized some impressive results, high-quality InAlN ternary is difficult to grow due to the fact that its immiscibility, phase separation and composition inhomogeneity always appear in the InAlN film.[9] In recent years, InAlGaN quaternary alloys have attracted considerable attention as a promising material to be used as the barrier.[10] As the Al/In ratio is 4.6, the InAlGaN can be grown lattice-matched to GaN.[11–13] With suitable Al/Ga ratio, InAlGaN quaternary is more miscible than $In_{0.18}Al_{0.82}N$. Moreover, such InAlGaN alloys offer a probability to independently adjust band-gap and strain state to some degree, which gives more flexibility in heterostructure design.[14]

In spite of the potential advantages of quaternary nitride compounds, there exist only a few reports on transistor structures and actual devices using InAlGaN-barriers.[15,16] Different from these reports, we have grown nearly lattice-matched InAlGaN/GaN heterostructures by employing pulsed metal organic chemical vapor deposition (PMOCVD). The use of PMOCVD allows us to reduce the growth temperature and hence significantly increases the indium incorporation to obtain high quality InAlGaN layers.[17–19] Furthermore, PMOCVD increases the surface mobility of adatoms and enables them to find energetically favorable sites, and hence improves the material composition uniformity. In this Letter, we present the results of nearly lattice-matched InAlGaN/GaN heterostructures grown by PMOCVD, as well as the performances of the HEMTs fabricated on this heterostructure.[13]

InAlGaN/GaN heterostructures were grown on 2 inch sapphire (001) substrates in a homemade vertical low pressure MOCVD system. Trymethylgallium (TEGa), trymethylaluminum (TMAl), trymethylindium (TMIn) and ammonia ($NH_3$) were used as precursors of Ga, Al, In, and N, respectively. Schematic diagram of InAlGaN/GaN heterostructure is shown in Fig. 1. The growth was initiated with an 80 nm AlN nucleation layer grown at 960℃, followed by an undoped 1.4 μm GaN buffer at 940℃. A ∼1 nm AlN interlayer was deposited at 940℃ on GaN buffer to improve the electron mobility by suppressing the alloy disorder scattering and enhancing the sheet carrier confinement. AlN (nucleation layer and interlayer) and GaN layers were grown by conventional continual MOCVD. After that, the growth temperature was cooled down to 720℃ for the growth of 20 nm InAlGaN barrier by PMOCVD. The reactive atoms were separately supplied to the reactor at

*Supported by the National Science and Technology Major Project of China under Grant No 2013ZX02308-002, and the National Natural Sciences Foundation of China under Grant Nos 61574108, 61334002, 61474086 and 61306017.

**Corresponding author. Email: jchzhang@xidian.edu.cn

© 2016 Chinese Physical Society and IOP Publishing Ltd

different times. The growth sequence of PMOCVD is described in Fig. 2. As it can be seen, there are two unit cells. Here 6 s pulses of TEGa, TMAl, $NH_3$ and 18 s pulse of TMIn were introduced alternately into the MOCVD reactor. An ammonia pulse always followed the metal-organic pulses. The growth parameters for InAlGaN quaternary have been optimized in an earlier publication.[17] The quaternary alloy compositions (In content of 16.62%, Al content of 73.15% and Ga content of 10.23%) were determined by X-ray photoelectron spectroscopy (XPS). At this composition, InAlGaN barrier is nearly lattice matched to the GaN channel. As the carrier gas, hydrogen was used for the growth of the AlN and GaN layers, and nitrogen for the InAlGaN barrier layer. After growth, the sample's structural properties were characterized by high resolution x-ray diffraction (HRXRD) and atomic force microscopy (AFM). Both van der Pauw–Hall and capacitance–voltage ($C$–$V$) measurements were carried out to investigate the electrical properties of InAlGaN/GaN heterostructure. Moreover, HEMTs with gate dimensions of $1 \times 50\,\mu m^2$ and 4 μm source–drain distance were fabricated on this heterostructure.

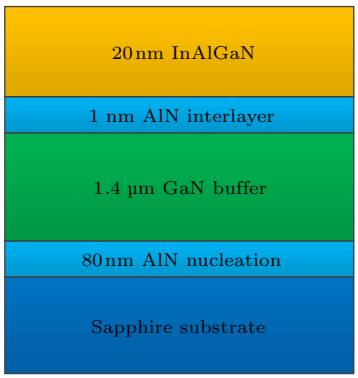


**Fig. 1.** Schematic diagram of InAlGaN/GaN heterostructure grown by PMOCVD.

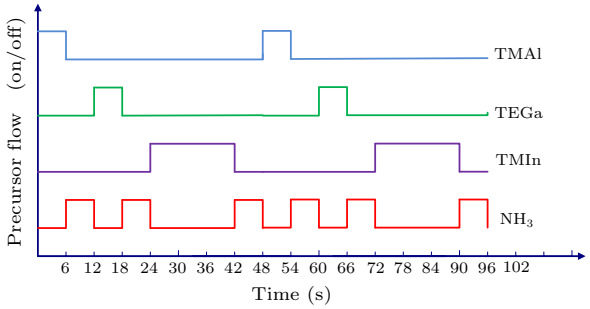


**Fig. 2.** Growth sequence of PMOCVD pulses for InAlGaN quaternary barrier.

Figure 3 shows the HRXRD $\omega$–$2\theta$ scan of InAlGaN/AlN/GaN heterostructure with InAlGaN thickness of 20 nm. There are mainly three diffraction peaks. The sharp peak of the GaN (002) located at 34.6° indicates the high crystal quality of the GaN buffer, the peak located at 36.2° corresponds to the AlN nucleation layer and the broad peak between them is the InAlGaN barrier (002) diffraction peak which indicates that there is no phase separation.

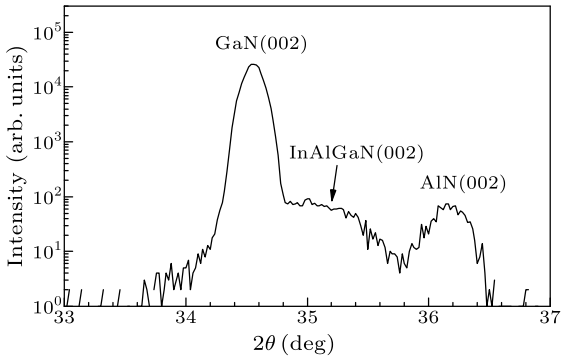


**Fig. 3.** HRXRD (002) $\omega$–$2\theta$ scan of InAlGaN/AlN/GaN heterostructures grown by PMOCVD

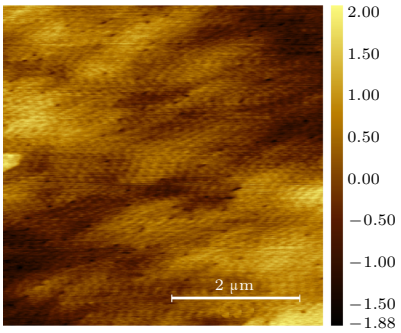


**Fig. 4.** AFM image of nearly lattice-matched InAlGaN/AlN/GaN surface morphology with a $5 \times 5\,\mu m^2$ scan area.

Figure 4 shows a typical AFM image with a $5 \times 5\,\mu m^2$ scan area taken from the InAlGaN barrier layer terminated surface in the nearly lattice-matched InAlGaN/GaN heterostructure. The image clearly shows a smooth surface morphology with atomic steps and a few pits that correspond to the dislocations extending from the GaN buffer layer. The surface morphology is similar to that observed for the AlGaN/GaN HFET structures. The rms surface roughness was measured to be approximately 0.62 nm, suggesting that the PMOCVD can lead to a monatomic smooth layer for thin InAlGaN film.

Carrier concentration distribution in the InAlGaN/AlGaN/GaN heterostructure was carried out by the $C$–$V$ measurements and the results are plotted in Fig. 5. It is observed that with the increase of the bias voltage, the capacitance plateaus appears at the pinch-off voltages of −5.4 V, which corresponds to the decrease amount and complete depletion of the confined two-dimensional electron gas (2DEG) density. The 2DEG peaks are sharp, with carrier concentrations of $9.2 \times 10^{19}\,cm^{-3}$ located at the position 21 nm below the surface of the sample, which includes a 20 nm InAlGaN barrier and a 1 nm AlN interlayer. From the Hall measurements using van der Pauw ge-

ometry, the 2DEG density is $1.43\times10^{13}\,\mathrm{cm}^{-2}$ with an electron mobility of $1668.08\,\mathrm{cm}^2/\mathrm{V{\cdot}s}$ at room temperature and the sheet resistance is $262.01\,\Omega/\square$. It should be noticed that the electron mobility is higher and the electron sheet carrier density is smaller than the previously reported values of nearly lattice-matched InAlN ternary in our laboratory.[13] The increase of the electron mobility is attributed to the optimization of growth parameters and the increase of the InAlGaN quaternary crystal quality, the decrease of the electron sheet carrier density is mainly due to the decrease of the spontaneous polarization electric field caused by the reduction of the Al content in the InAlGaN quaternary barrier layer.

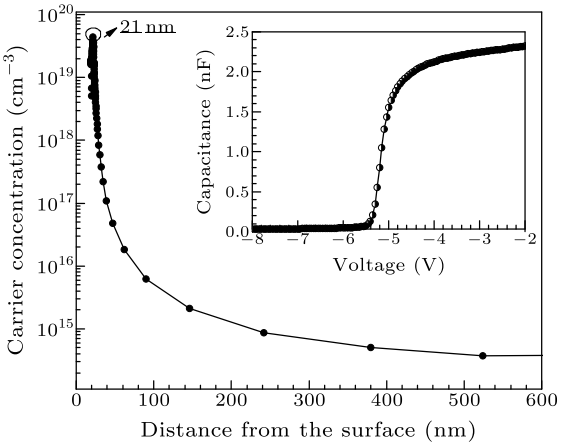


**Fig. 5.** The $C$–$V$ measurement curves of nearly lattice-matched InAlGaN/AlN/GaN heterostructures grown by PMOCVD.

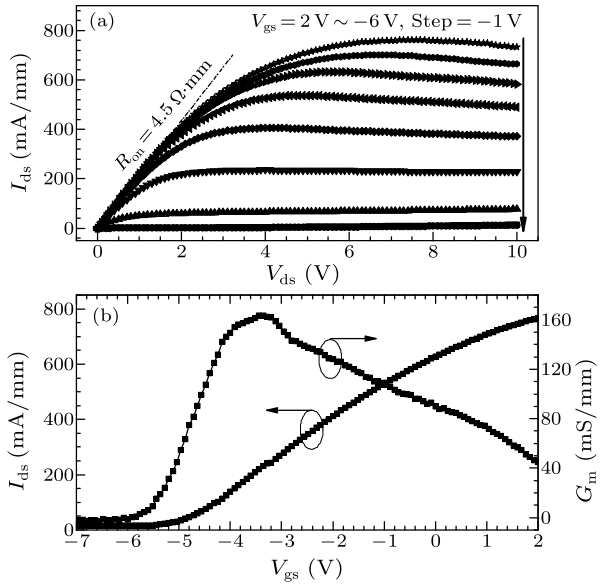


**Fig. 6.** Direct current characteristics of InAlGaN/ GaN HEMT with gate dimensions of $1\times50\,\mu\mathrm{m}^2$: (a) common-source $I$–$V$ measured from $V_{gs}=+2\,\mathrm{V}$ to $-6\,\mathrm{V}$ in steps of $-1\,\mathrm{V}$, (b) transfer characteristics measured at $V_{ds}=10\,\mathrm{V}$, $V_{gs}=-10\,\mathrm{V}$–$2\,\mathrm{V}$ in steps of $1\,\mathrm{V}$.

The HEMTs devices with dimensions of $1\times50\,\mu\mathrm{m}^2$ and $4\,\mu\mathrm{m}$ source–drain distance were fabricated on this nearly lattice-matched InAlGaN/AlN/GaN heterostructures. Figure 6 presents the common-source $I$–$V$ characteristics. The gate–source bias $V_{gs}$ was stepped from $+2\,\mathrm{V}$ to $-6\,\mathrm{V}$ and the gate–drain bias $V_{ds}$ was swept from 0 to $10\,\mathrm{V}$. At $V_{gs}=2\,\mathrm{V}$, a maximum output current density $I_{dsmax}$ of $763.91\,\mathrm{mA/mm}$ is reached, and the on-resistance $R_{on}$ is calculated to be $4.5\,\Omega{\cdot}\mathrm{mm}$ in the linear region, and a maximum extrinsic transconductance of $163.13\,\mathrm{mS/mm}$ is achieved at $V_{ds}=10\,\mathrm{V}$.

Small-signal rf measurements were taken from $100\,\mathrm{MHz}$ to $110\,\mathrm{GHz}$ with an Agilent E8363B vector network analyzer calibrated by using line-reflect-reflect-match off-wafer impedance standards. The deem-bedded current gain $|h_{21}|^2$ and the maximum available power gain (MAG) are plotted in Fig. 7, as a function of frequency at the peak $G_m$ bias condition of $V_{ds}=10\,\mathrm{V}$ and $V_{gs}=-3.3\,\mathrm{V}$. The extrapolation of $|h_{21}|^2$ and MAG at a $-20\,\mathrm{dB/dec}$ slope gives $f_T/f_{max}$ of 11/21 GHz, which corresponds to a relatively high $f_T\times L_g$ of $11\,\mathrm{GHz{\cdot}\mu m}$. Further improvement of output current and frequency performance can be achieved by scaling down the gate length and further optimization of growth.

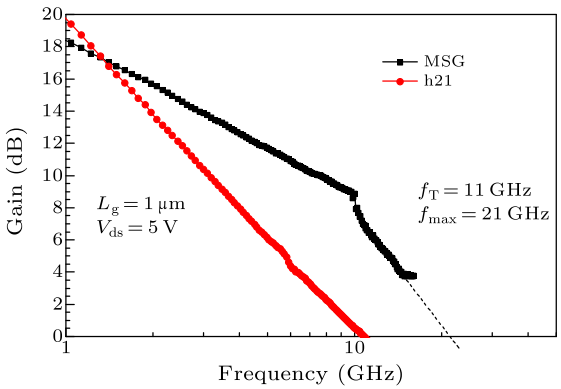


**Fig. 7.** Current-gain and power-gain cut-off frequencies at $V_{ds}=5\,\mathrm{V}$ of a $1\times50\,\mu\mathrm{m}^2$ InAlGaN/GaN HEMT.

In summary, InAlGaN/GaN heterostructure fabricated on sapphire (001) substrates by PMOCVD and its structural and electrical properties have been investigated. A smooth surface with rms roughness of $0.62\,\mathrm{nm}$ is obtained from the nearly lattice-matched InAlGaN/GaN heterostructures. The electron mobility is $1668.08\,\mathrm{cm}^2/\mathrm{V{\cdot}s}$ with a high 2DEG density of $1.43\times10^{13}\,\mathrm{cm}^{-2}$ at room temperature. The HEMTs with gate dimensions of $1\times50\,\mu\mathrm{m}^2$ exhibit a maximum drain current of $763.91\,\mathrm{mA/mm}$ and a maximum extrinsic transconductance of $163.13\,\mathrm{mS/mm}$. Good frequency response is achieved with $f_T$ of $11\,\mathrm{GHz}$ and $f_{max}$ of $21\,\mathrm{GHz}$. The results demonstrate the promising potential of the PMOCVD growth method for InAlGaN/GaN millimeter wave power electronics applications. To further improve the performances of the devices, growth parameters optimization of PMOCVD

such as growth temperature and Al/Ga ratio should be pursued to enhance the crystal quality of the InAlGaN quaternary barrier and electrical properties of the InAlGaN/GaN heterostructures.

## References


[1] Steven C B, Kiki I, Jason A R, Walter K, Doewon P, Harry B D, Daniel D K, Alma E W and Richard L H 2001 *IEEE Trans. Electron Devices* **48** 465

[2] Wu Y F, Ibbetson J P, Parikh P, Keller B P, Mishra U K and Kapolnek D 2001 *IEEE Trans. Electron Devices* **48** 586

[3] Liu Y, Egawa T, Ishikawa H and Jimbo T 2003 *J. Cryst. Growth* **259** 245

[4] Wu J J, Li D B, Lu Y, Han X X, Li J M, Wei H Y, Kang T T, Wang X H, Liu X L, Zhu Q S and Wang Z G 2004 *J. Cryst. Growth* **273** 79

[5] Goto O, Tomiya S, Hohshina Y, Tanaka T et al 2007 *Proc. SPIE* **6485** 64850Z

[6] Kuzmík J 2001 *IEEE Electron Device Lett.* **22** 510

[7] Jeganathan K, Shimizu M, Okumura H, Yano Y and Akutsu N 2007 *J. Cryst. Growth* **304** 342

[8] Gonschorek M, Carlin J F, Feltin E, Py M A and Grandjean N 2006 *Appl. Phys. Lett.* **89** 062106

[9] Schenk H P D, Nemoz M, Korytov M, Vennéguès P, Dräger A D and Hangleiter A 2008 *Appl. Phys. Lett.* **93** 081116

[10] Wang R H, Li G W, Verma J, Berardi S R, Fang T, Guo J, Hu Z Y, Laboutin O, Cao Y, Johnson W, Snider G, Fay P, Jena D and Xing H L 2011 *IEEE Electron Device Lett.* **32** 1215

[11] Nakazawa S, Ueda T, Inoue K, Tanaka T, Ishikawa H and Egawa T 2005 *IEEE Trans. Electron Devices* **52** 2124

[12] Lim T, Aidam R, Kirste L, Waltereit P, Quay R, Müller S and Ambacher O 2010 *Appl. Phys. Lett.* **96** 252108

[13] Xue J S, Hao Y, Zhang J C, Zhou X W, Liu Z Y, Ma J C and Lin Z Y 2011 *Appl. Phys. Lett.* **98** 113504

[14] Benjamin R, Wille A, Ketteniss N, Hahn H, Hollander B, Heuken M, Kalisch H and Vescan A 2013 *J. Electron. Mater.* **42** 826

[15] Wang R H, Li G W, Karbasian G, Guo J, Song B, Yue Y Z, Hu Z Y, Laboutin O, Cao Y, Johnson W, Snider G, Fay P, Debdeep J and Xing H L 2013 *IEEE Electron Device Lett.* **34** 378

[16] Ketteniss N, Khoshroo L R, Eickelkamp M, Heuken M, Kalisch H, Jansen R H and Vescan A 2010 *Semicond. Sci. Technol.* **25** 075013

[17] Quan R D, Zhang J C, Xu S R, Xue J S, Zhao Y, Ning J, Lin Z Y, Ren Z Y and Hao Y 2016 *Chin. Phys. Lett.* **33** 048101

[18] Xue J S, Hao Y, Zhou X W, Zhang J C, Yang C K, Ou X X, Shi L Y, Wang H, Yang L A and Zhang J F 2011 *J. Cryst. Growth* **314** 359

[19] Xue J S, Zhang J C and Hao Y 2014 *J. Cryst. Growth* **401** 661